International Journal of Pharmaceutics 477 (2014) 408–415

Contents lists available at ScienceDirect

International Journal of Pharmaceutics

journal homepage: www.elsevier.com/locate/ijpharm

Pharmaceutical nanotechnology

The enhanced longevity and liver targetability of Paclitaxel by hybrid liposomes encapsulating Paclitaxel-conjugated gold nanoparticles

Quan-Ying Bao [a], Ning Zhang [a], Dong-Dong Geng [a], Jing-Wei Xue [a], Mackenzie Merritt [b], Can Zhang [a], Ya Ding [a,*]

[a] Key Laboratory of Drug Quality Control and Pharmacovigilance, China Pharmaceutical University, Ministry of Education, Nanjing 210009, China
[b] Department of Biology, Faculty of Science, University of Waterloo, Waterloo, Ontario N2L 3G1, Canada

ARTICLE INFO

Article history:
Received 31 August 2014
Received in revised form 30 September 2014
Accepted 15 October 2014
Available online 18 October 2014

Keywords:
Hybrid liposomes
Gold conjugates
Paclitaxel
Pharmacokinetics
Biodistribution
Anticancer efficacy

ABSTRACT

Organic and inorganic drug delivery systems both demonstrate their own advantages and challenges in practical applications. Combining these two drug delivery strategies in one system is expected to solve their current issues and achieve desirable functions. In this paper, gold nanoparticles (GNPs) and liposomes have been chosen as the model systems to construct a hybrid system and investigate its performance for the tumor therapy of Paclitaxel (PTX). The thiol-terminated polyethylene glycol (PEG_{400})–PTX derivative has been covalently modified on the surface of GNPs, followed by the encapsulation of PTX-conjugated GNPs (PTX–PEG_{400}@GNPs) in liposomes. The hybrid liposomes solve the solubility and stability problems of gold conjugates and show high drug loading capacity. *In vitro* PTX release from the hybrid system maintains the similar sustained behavior demonstrated in its conjugates. Under the protection of a biocompatible liposome shell, encapsulated PTX shows enhanced circulation longevity and liver targetability compared to Taxol® and PTX–PEG_{400}@GNPs suspension in the pharmacokinetic and biodistribution studies. These indicate that encapsulating drug-conjugated inorganic nanoparticles inside organic carriers maintains the superiority of both vehicles and improves the performance of hybrid systems. Although these attributes of hybrid liposomes lead to a better therapeutic capacity in a murine liver cancer model than that of the comparison groups, it shows no significant difference from Taxol® and conjugate suspension. This result could be due to the delayed and sustained drug release from the system. However, it indicates the promising potential for these hybrid liposomes will allow further construction of a compound preparation with improved performance that is based on their enhanced longevity and liver targetability of Paclitaxel.

1. Introduction

With the recent advances of nanotechnology in drug delivery, it has become increasingly possible to address some of the issues associated with previously approved drugs and new molecular entities, such as poor water solubility, a very short circulating half-life, and a serious systematic toxicity (Sinha et al., 2006). A large number of natural and synthetic carriers have been exploited at the nanoscale for the transportation of pharmaceutical compounds in the body as needed to safely achieve their desired therapeutic effect (Farokhzad and Langer, 2009; Bertrand et al., 2014). According to the manner in which the drug is incorporated with the carrier, these nanovehicles can be mainly divided into two categories, encapsulating and encapsulated, both having their own advantages and challenges.

"Encapsulating" refers to a variety of "soft" lipid or polymer carriers that encapsulate pharmaceutical compounds in their hydrophobic core and stabilize the whole system with a hydrophilic shell. This includes micelles, liposomes (Lips), polymersomes, dendrimers, and nanoparticles (Kataoka et al., 2001; Torchilin, 2005 Wu et al., 2014). Drug molecules are protected in the carrier in their active forms to solve poor water solubility, blood stability, and burst release problems. However, low drug payloads, undesired drug leakage before reaching the target, and clearance by the reticuloendothelial system (RES) remain challenging problems for clinical applications.

The "encapsulated" category includes a series of "hard" inorganic nanomaterials or their oxides, such as carbon nanotubes

* Corresponding author. Tel.: +86 25 83271326; fax: +86 25 83271326.
E-mail address: ayanju@163.com (Y. Ding).

http://dx.doi.org/10.1016/j.ijpharm.2014.10.040
0378-5173/

(Liu et al., 2008), silica nanoparticles (Jang et al., 2013), quantum dots (Chakravarthy and Davidson, 2011), gold nanoparticles (GNPs) (Daniel and Astruc, 2004), and iron oxide nanoparticles (Liao et al., 2011). In contrast to organic vehicles that self-assemble *via* hydrophilic and hydrophobic interactions in solution, inorganic nanomaterials commonly conjugate drug molecules or their derivatives on the particle surface through covalent connections. This means that the nanocarriers are encapsulated by an organic shell composed of specific targeting and drug payloads. High stability *in vivo* due to core crosslinking structure of nano-prodrug and enhanced efficacy due to clathrin-mediated endocytosis make these materials attractive for fabricating multifunctional nanocarriers for both chemotherapy and gene therapy (Liang et al., 2014; Ding et al., 2014a). Although hydrophilic polymers, such as polyethylene glycol (PEG), have been simultaneously conjugated on the particle surface, the hydrophobicity of therapeutic molecules decreases the system's water solubility and dispersion. In addition, the drug molecule is easily recognized and degraded by various proteins and enzymes in the physiological environment because it is located on the surface of the whole system. These processes may reduce the blood concentration and circulation time of therapeutics, along with the drug levels in tumor tissues.

The combination of these two strategies in one system is expected to achieve complementary advantages and improve the performance of the well-designed drug delivery system (DDS). However, current research focuses on co-encapsulating drug and inorganic materials simultaneously in thermosensitive organic carriers to achieve the molecular imaging and photothermal therapy properties of a combinative system (Oh et al., 2014; Gui et al., 2014; Rengan et al., 2014). There are few reports of the pharmaceutical property improvement of combinative DDSs based on their natural merits.

In our previous work to improve the performance of Paclitaxel (PTX), a series of mercapto group-terminated PEG–PTX ligands had been designed and synthesized to fabricate PTX-conjugated GNPs (PTX–PEG@GNPs) (Ding et al., 2013). The PEG MW is adjusted from 400 to 1000 Da to increase water solubility and simultaneously minimize the size of the gold conjugates. Although significant improvement of therapeutic efficacy for this conjugate has been demonstrated in a murine liver cancer model, there are still two issues that need to be solved. Firstly, the drug location in the outmost layer of conjugates leads to low stability in particle dispersion, due to the hydrophobic interactions between PTX molecules, and in biological activity, caused by enzyme degradation *in vivo*. Secondly, although the PEG MW of 1000 Da is enough to increase the solubility of PTX in PTX–PEG@GNPs (184 mg/mL), PEG spacer with less molecular weight (such as 400 and 600 Da) results in the poor solubility of as-prepared PTX–PEG@GNPs in water. In addition, based on our previous studies, the spacer with a short chain, such as PEG_{400}, decreases the size of the gold conjugates, and also renders its conjugate particles more efficient at tumor cellular uptake than other spacers with larger molecular weights (Ding et al., 2014b). Therefore, encapsulating conjugate nanoparticles inside lipid or polymeric carriers is expected to solve the solubility and stability issues and maintain the superiority of gold conjugates simultaneously.

In the present work, liposomes and GNPs are employed as model systems to fabricate a hybrid carrier. A liposome is an artificially-prepared spherical vesicle composed of a lipid bilayer. Lips have been widely used in the biotechnology and pharmaceutical industries in the past decades as a robust biomembrane DDS (Derycke and Witte, 2004; Lasic and Templeton, 1996). Here, the mercapto group-terminated PEG ligand of PTX (PTX–PEG_{400}–SH) is covalently coupled with GNPs, and then the as-prepared PTX–PEG_{400}@GNPs are encapsulated in liposomes to fabricate hybrid liposomes (PTX–PEG_{400}@GNP–Lips). In contrast to previous studies, both liposomes and GNPs act as drug carriers and contribute their drug delivery strengths in the combinative system. The property and performance improvement for the combination of "encapsulating" and "encapsulated" strategies in DDSs is investigated. The detailed characterization of the structure and pharmaceutical properties of hybrid liposomes has been carried out. Their tumor treatment efficacy in the tumor bearing mouse models is then systematically investigated and compared to the commercial PTX formulation (Taxol®) and gold conjugates without liposome protection (PTX–PEG_{400}@GNPs).

2. Materials and methods

2.1. Materials

Hydrogen tetrachloroaurate hydrate ($HAuCl_4 \cdot 3H_2O$) was obtained from Shanghai Chemical Regent Company (China). PTX (97%) was purchased from Jiangsu Yew Pharmaceutical Co., Ltd (China). Soy Lecithin (SPC, S100) was obtained from GmbH Lipoid (Ludwigshafen, Germany). Cholesterol was purchased from Shanghai Huixing Biochemical Reagent Co., Ltd. (China). Unless otherwise stated, all the starting materials were obtained from commercial suppliers and used without further purification. All aqueous solutions were prepared using deionized water (>18 MΩ, Purelab Classic Corp., USA).

2.2. Preparation of citrate-protected GNPs

Citrate-protected GNPs were synthesized in a single-phase system (Ding et al., 2007, 2009) by filtering sub-boiling water through a microporous membrane with an aperture of 0.22 μm. All the glasswares were cleaned in a bath of freshly prepared aqua regia and rinsed thoroughly with deionized water prior to use. $HAuCl_4 \cdot 3H_2O$ (0.615 mL, 0.02 g/mL) and sodium citrate (50 mg, 1.3 mmol) were dissolved in 50 mL of triply distilled H_2O. A freshly prepared and cooled aqueous solution of sodium borohydride (1.2 mL, 0.1 M) was added to the reaction solution, resulting in an immediate color change to pink. After vigorous stirring for 30 min, the resulting solution appeared as a burgundy-red colloidal dispersion of gold.

2.3. Synthesis of therapeutic ligand (PTX–PEG_{400}–SH)

The synthesis and characterization of PTX–PEG_{400}–SH ligand and its intermediates were referenced in our previous report (Ding et al., 2013).

2.4. Preparation of PTX–PEG_{400}@GNP conjugates

720 mg of PTX–PEG_{400}–SH (0.5 mmol) was dissolved in 6.7 mL of methanol by magnetic stirring at room temperature. Citrate-protected GNPs (5.35 mL) were added to the solution of PTX–PEG–SH drop wise. After the mixture was stirred for 1 h, the cream-like precipitation of the reaction was dried under vacuum. The gold conjugates were then purified by gel separation chromatograpy using a Sephadex (G-25) gel column as the stationary phase and methanol: H_2O (30:70 v/v) as the mobile phase. After the collection of a solution with a light reddish-brown color and evaporating the organic solvent under vacuum, the product is obtained through the freeze drying method.

2.5. Preparation of PTX–PEG_{400}@GNP–Lips

The thin film hydration method (Samad et al., 2007) was adopted to prepare the hybrid liposomes. 100 mg of SPC, 25 mg of cholesterol, and 20 mg of PTX–PEG_{400}@GNPs were dissolved with

4 mL chloroform in a 500 mL round bottom flask. The chloroform was removed by using a vacuum rotary evaporator at 37 °C, forming a thin film of lipid at the wall of the flask. The lipid film was rehydrated with 10 mL saline for 30 min to obtain large unilameller vescicles, which were then sonicated for 70 min at 16% power (total 650 W) in an ice–water bath. The as-prepared liposomes were stocked at 4 °C.

2.6. Characterization

Ultraviolet-visible (UV–vis) spectra were measured with a UV-2401 PC UV/Vis spectrophotometer (Shimadzu, USA). The diameter, dispersity, and Zeta potentials of the blank and hybrid liposomes were measured using a Zetasizer 3000HS instrument (Malvern Instruments, Malvern, UK) with 633 nm He–Ne lasers at 25 °C, while the lyophilized powder was reconstituted with double distilled water. A single drop of each solution was deposited on a transmission electron microscopy (TEM) grid and allowed to air dry. All the samples were imaged using a JEM-200CX TEM (JEOL) with an acceleration voltage of 200 kV. Thermogravimetric analysis (TGA) was performed using a thermal gravimetric analyzer (TG 209 F1, Netzsch, Germany).

The analysis of PTX and its therapy ligand (PTX–PEG_{400}–SH here) was performed on a reversed-phase high performance liquid chromatography (RP-HPLC) system with UV detection at 227 nm. The HPLC system was Shimadzu LC-20A series (Shimadzu Corporation, Japan), consisting of a quaternary pump, a vacuum degasser, an auto-sampler, a thermostated column compartment, and an analytical column C18 (BDS HYPERSIL, 250 mm × 4.6 mm, ID 5 μm; Thermo Inc., USA). The column temperature was set at 35 °C with an isocratic elution at a flow rate of 1.0 mL/min and the injection volume was 20 μL. The mobile phase was 75% (v/v) methanol.

2.7. In vitro *drug release of PTX–PEG_{400}@GNP–Lips*

1 mL of the PTX–PEG_{400}@GNP–Lips was placed in a dialysis tube (MWCO = 10,000 Da), which was sealed with cable ties and immersed into 10 mL of release media at 37 ± 0.5 °C in a beaker. This study adopted three different Tween 80 (0.1%, w/w) aqueous release media with or without addition of 10 mM glutathione (GSH) or GSH plus pig liver esterase (20 units). At predetermined time points, 200 μL of samples were withdrawn and replenished with 200 μL of fresh release media. All the samples were performed in triplicates.

2.8. Pharmacokinetic studies

2.8.1. Experimental design

Male Sprague Dawley (SD) rats weighing 240 ± 20 g were divided into two groups ($n = 3$) and administered Taxol®, sodium carboxyl methyl cellulose (CMC-Na) suspension of PTX–PEG_{400}@GNPs, and PTX–PEG_{400}@GNP–Lips at a dose of 7 mg/kg *via* tail vein injection, respectively. 0.5 mL of blood samples were withdrawn from retro orbital sinus at 0.083, 0.17, 0.25, 0.5, 1, 2, 4, 6, 8, 10, 12, 24, 36, and 48 h after injection. The blood samples were collected in heparinized tubes and centrifuged at 8000 rpm for 10 min. The plasma samples were separated and stored at −20 °C until the assay.

2.8.2. Sample preparation and analysis

For a 100 μL aliquot of each plasma sample, 200 μL of acetonitrile was added and vortex mixed for 3 min. The sample was centrifuged at 15,000 rpm for 10 min. 20 μL of the supernatant of each sample was injected for validated HPLC analysis. The calibration curve was set at the level of 0.1–20 μg/mL ($r^2 = 0.9997$), and the HPLC condition was the same as the *in vitro* PTX analysis in Section 2.6.

2.9. Biodistribution

2.9.1. Animal experiment

60 healthy male ICR (imprinting control region) mice (body weight 20 ± 2 g) were divided into three groups, and administered Taxol®, PTX–PEG_{400}@GNP suspension, and PTX–PEG_{400}@GNP–Lips at a dose of 7 mg/kg by tail vein, respectively. The blood samples were collected at 1, 2, 4, 8, and12 h following administration, after which the mice were sacrificed to excise heart, liver, spleen, lung, and kidney, all of which were washed with saline and weighed before sample preparation.

2.9.2. Sample preparation and analysis

100 μL of the blood samples were dealt with 200 μL acetonitrile to precipitate proteins, and centrifuged at 15,000 rpm for 10 min. 20 μL of the upper supernatant was assayed by HPLC. All the tissues were homogenized with 800 μL of saline, and 200 μL of the homogenate was deproteinized by 200 μL acetonitrile and centrifuged at 15,000 rpm for 10 min. 20 μL of the supernatant was analyzed *via* validated HPLC. The calibration curves of both tissues and blood displayed good linearity.

2.10. In vivo *antitumor efficacy*

2.10.1. Animal experiment

Healthy male ICR mice were randomly divided into four goups ($n = 5$) and 100 μL of carcinoma Heps buffer (1×10^7/mL) was implanted into the flank of each mouse. The tumor width (W) and length (L) were measured after implantation and the tumor size or volume (V) was calculated by the following formula: $V = (W^2 \times L)/2$ (Liu et al., 2011). When the tumor volume was approximately 100–200 mm^3, Saline, Taxol®, PTX–PEG_{400}@GNPs suspension and PTX–PEG_{400}@GNP–Lips were respectively injected *via* tail vein at a dose of 7 mg/kg at 0 (the first day of drug administration), 2, 4, 6, and 8 day time points. Meanwhile, the weight and volume of each mouse were recorded accordingly. After the last drug administration, the mice were sacrificed and the tumors were excised and weighed.

2.10.2. Histological analysis of tumors

The tumors were immersed into 4% formalin, sectioned and stained with hematoxylin and eosin (H&E) for histological observation (Olympus TH4-200, Olympus Optical Co., Ltd., Japan).

2.11. Statistics

All the results are presented as mean ± SD. The data were analyzed by one-way analysis of variance (ANOVA) with the appropriate Bonferroni correction to determine the significant differences *via* OriginPro (Verison 8.6) for multiple comparisons. Significance was assumed at $P < 0.05$.

3. Results and discussion

3.1. Preparation and characterization of PTX–PEG_{400}@GNPs and PTX–PEG_{400}@GNP–Lips

The composition and structure of PTX–PEG_{400}@GNPs and their hybrid liposomes are illustrated in Fig. 1. The synthesis method for the thiol-terminated PEG–PTX ligands (with PEG MW = 400 Da) is

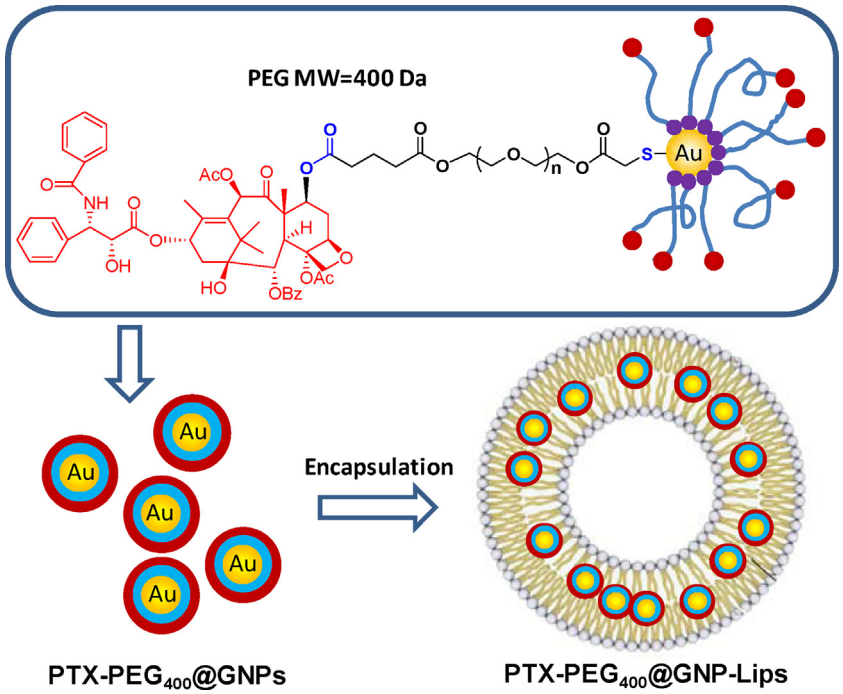

Fig. 1. The chemical structure of PTX-conjugated GNPs (PTX–PEG_{400}@GNPs) and composition illustration of their encapsulated liposomes (PTX–PEG_{400}@GNP–Lips).

covered in our previous report (Ding et al., 2013). The gold conjugate is prepared through the ligand exchange reaction on the surface of citrate-protected GNPs. The PTX–PEG_{400}@GNPs were insoluble in water, but they easily dissolved in organic solvents such as chloroform and dimethyl sulfoxide. In order to solve the problem of solubility and increase the stability and bioavailability of antitumor drugs in the conjugates simultaneously, PTX–PEG_{400}@GNPs are encapsulated in the liposomes by using the thin-film dispersion method (Liu et al., 2011). The prepared hybrid liposomes can disperse well in water, appearing as a white opalescent solution with a light brown color.

The UV–vis spectra of citrate-protected GNPs, PTX–PEG_{400}@GNPs, and PTX–PEG_{400}@GNP–Lips are presented in Fig. 2A. Compared with the sodium citrated stabilized GNPs (curve a), the absorption peak of PTX–PEG_{400}@GNPs appears at the same wavelength of 520 nm (curve b). The absorption spectrum of

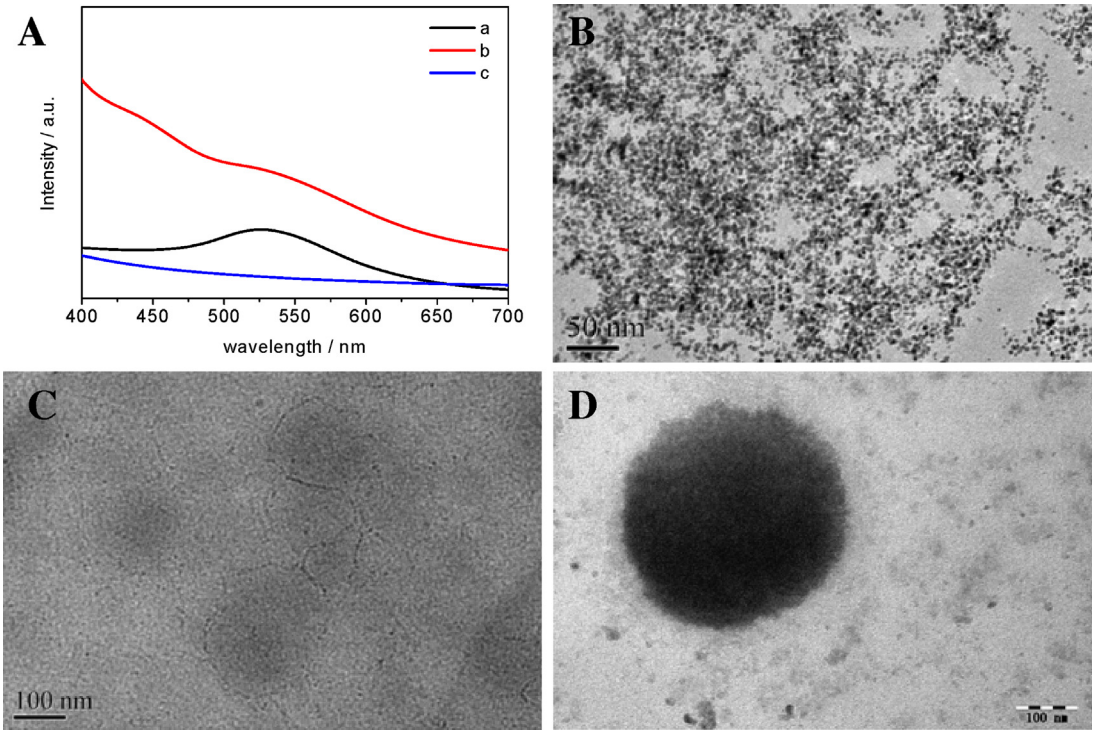

Fig. 2. (A) UV–vis spectra of citrate-protected GNPs (curve a), PTX–PEG_{400}@GNPs (curve b), and PTX–PEG_{400}@GNP–Lips (curve c), and TEM images of (B) PTX–PEG_{400}@GNPs, (C) blank liposomes, and (D) PTX–PEG_{400}@GNP–Lips.

PTX–PEG_{400}@GNP–Lips is shown in Fig. 2A, curve c. Due to the white opalescent solution of liposomes, the surface plasmon resonance (SPR) of gold around 520 nm cannot be observed. To investigate the size and morphology of particles and their hybrid liposomes, TEM images of PTX–PEG_{400}@GNPs, blank liposomes, and PTX–PEG_{400}@GNP–Lips are displayed in Fig. 2B–D. The particle size of PTX–PEG_{400}@GNPs is shown to be ca. 3.41 ± 0.36 nm gold core (counting and calculating with 100 particles). While some particles dispersed well, the surfaces of other particles adhered to one another due to the solvent evaporation (Fig. 2B). This can be a result of the hydrophobic interaction between PTX located on different particle surfaces. In the TEM images of Fig. 2C, only fuzzy aggregates around 150 nm can be observed for blank liposome samples without staining. After loading heavy metal particles such as PTX–PEG_{400}@GNPs in our study, the black spherical liposomes in the images could be observed clearly (Fig. 2D). Black dots in the images of PTX–PEG_{400}@GNP–Lips were PTX–PEG_{400}@GNPs, which shows the successful encapsulation of gold conjugates into the bilayer of liposomes. As a result of the high loading density and 3D arrangement of gold conjugates inside the liposomes, the hollow cores of the liposomes were not very obvious. Furthermore, the hydrodynamic diameters and Zeta potentials of PTX–PEG_{400}@GNP–Lips were determined using dynamic light scattering (DLS) measurements to be 281.1 ± 5.4 nm and 45.33 ± 4.51 mV, respectively.

3.2. Drug loading capacity (DLC) of PTX–PEG_{400}@GNPs and PTX–PEG_{400}@GNP–Lips

To determine the DLC of PTX–PEG_{400}@GNPs and their hybrid liposomes, drug content on the surface of gold conjugates was measured by using the TGA method and the therapeutic ligand in liposomes was detected *via* GSH exchange and subsequent HPLC methods. The weight loss graph of PTX–PEG_{400}@GNPs after purification is shown in Fig. 3. From the results, the weight loss of the organic layer of the conjugate is about 84%. The calculation of DLC for gold conjugates is according to the equation: DLC% = the weight of drug in conjugate/the weight of conjugate × 100% (Ding et al., 2013). Based on the molecular weight of PTX being 853.92 g/mol and its PEG ligand being 1423 g/mol, the content of PTX in PTX–PEG_{400}@GNPs was calculated to be 50.4%.

The DLC value for the hybrid liposomes is difficult to determine directly by using a simple method. Therefore, PTX ligands that were conjugated with GNPs and then encapsulated in liposomes were detected by using GSH exchange and a subsequent HPLC method (n = 3). Firstly, the demulsification of liposomes was carried out by the addition of methanol to the liposome solution. GSH solution (10 mM) was then added to the solution and left to stir at room temperature and exchange the PTX–PEG_{400}–SH ligand for 6 days. Finally, the concentration of the ligand was detected using the HPLC method. The content of PTX encapsulated in the PTX–PEG_{400}@GNP–Lips can be calculated to be 1.064 mg/mL. This result indicates that almost all PTX–PEG_{400}@GNPs were encapsulated in liposomes in the preparation process. Therefore, the DLC of liposomes (DLC% = drug in liposomes/(drug + carrier in liposomes)) can be calculated to be 7.9% (w/w).

3.3. In vitro *release studies*

It has been proven that, due to a special chemical structure design, the as-prepared gold conjugate presents a dual and simultaneous stimulation-induced drug release behavior in the presence of both esterase and high concentrations of glutathione (Ding et al., 2013). To investigate the *in vitro* release of PTX and its derivative from PTX–PEG_{400}@GNP–Lips, this study adopted three different aqueous release media, including phosphate buffer solutions (PBS, pH 7.4) after adding Tween 80 (0.1% w/w), Tween 80 plus 10 mM GSH, and Tween 80 with 10 mM GSH plus pig liver esterase (20 units). In the medium of Tween 80 alone, no drug molecules or thiol-terminated PEG derivatives were detected in 6 days (data not shown here). This result indicates high stability of hybrid liposomes in PBS at physiological pH.

The release profile of the drug from PTX–PEG_{400}@GNP–Lips in the GSH plus Tween 80 release medium is presented in Fig. 4. Considering both the PTX and PTX–PEG_{400}–SH have the possibility to release from the PTX–PEG_{400}@GNP–Lips, both of the forms were assayed. The release profile illustrates that the absence of the esterase caused the parent drug PTX to be nearly non-releasing. In contrast to the PTX–PEG_{1000}@GNPs, the mercapto-terminal PEG–PTX ligand is released gradually from hybrid liposomes due to the presence of GSH only. Although the release rate is very slow, near 50% of PTX–PEG_{400}–SH ligand was liberated in 144 h (6 days). The release rate is lower than the results of the DLC calculation, meaning the ligands release after the demulsification of hybrid liposomes. This phenomenon indicates that (1) with the PEG MW decreasing to 400 Da, the ligand is easier to displace from the gold surface than the one of PEG MW 1000 Da under the condition of high GSH concentration inside cells; (2) the encapsulation of

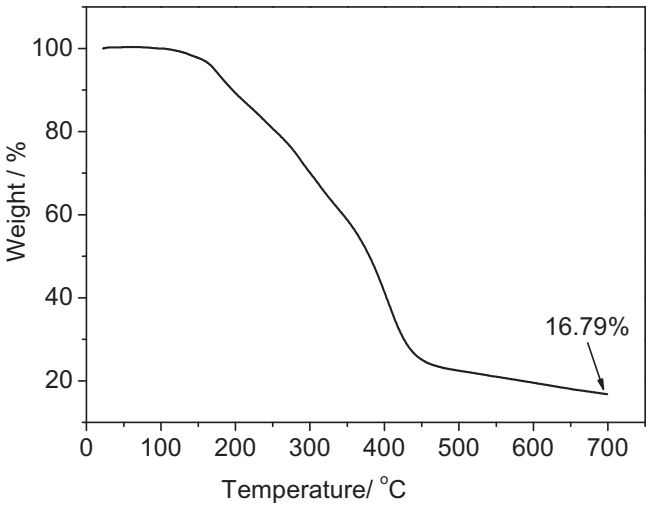

Fig. 3. TGA curve of PTX–PEG_{400}@GNPs.

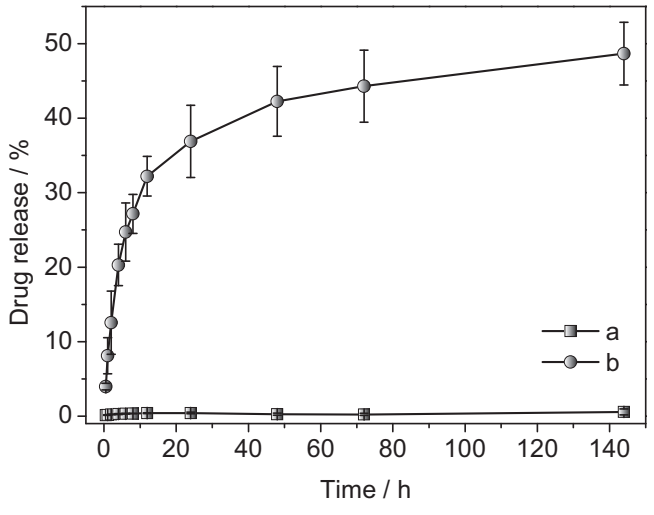

Fig. 4. The drug release profiles of PTX–PEG_{400}@GNP–Lips in the release media of Tween 80 with 10 mM of GSH: (a) PTX and (b) thiol-terminated PEG_{400}–PTX ligand.

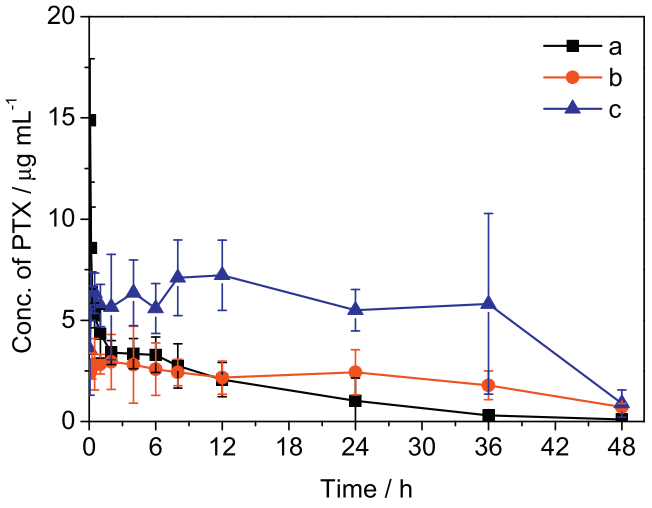

Fig. 5. The mean plasma concentration-time curves of (a) Taxol®, (b) PTX–PEG_{400}@GNPs CMC-Na suspension, and (c) PTX–PEG_{400}@GNP–Lips following intravenous administration at a dose of 7 mg PTX/kg in rats (mean ± SD, $n = 3$).

conjugates in liposomes will not inhibit the exchange reaction between GSH and a therapeutic ligand, but reduce the replacement rate; (3) the prolonged ligand release will be beneficial to the longevity design of the DDS because further drug release (above 50%) requires a longer period of time (more than 6 days).

Moreover, in the media containing pig liver esterase, the liposomes were decomposed and the dialysis tube became turbulent. The white precipitate mixed with the brown appeared quickly in the medium, and possibly includes the enzyme, composition materials of liposomes, and a brown slurry of gold conjugate. However, in the absence of esterase it was difficult to imitate an *in vivo* environment for the PTX release of hybrid liposomes. Therefore, the pharmacokinetic studies are carried out to investigate *in vivo* drug release and the stability of test samples.

3.4. Pharmacokinetics

Three formulations of PTX (Taxol®, PTX–PEG_{400}@GNPs CMC-Na suspension, and PTX–PEG_{400}@GNP–Lips) were tested in rats to detect the pharmacokinetic parameters. All the data were dealt with using Kentica 4.0. The time–concentration curve is displayed in Fig. 5. The Taxol® formulation, in which PTX is dissolved in Kolliphor EL and ethanol, demonstrated the lowest PTX plasma concentration in 48 h, thus, indicating rapid drug elimination in the body. In the case of PTX–PEG_{400}@GNPs CMC-Na suspension, due to the stability of chemical structure in conjugates and their intracellular drug release mechanism (Ding et al., 2013), the PTX plasma concentration after 12 h administration surpasses that of Taxol®. However, without the protection of liposomes, the results were still far lower than the PTX–PEG_{400}@GNP–Lips after 5 min of intravenous injection. This indicates the importance of a protective shell for the stability of gold conjugates. Compared with the curves of the other two formulations, PTX–PEG_{400}@GNP–Lips could obviously maintain the plasma concentration at a relatively steadier and higher level within 48 h. The plasma of PTX at 36 h for the PTX–PEG_{400}@GNP–Lip group was 18.8- and 3.2-fold the values of Taxol® and PTX–PEG_{400}@GNPs CMC-Na suspension, respectively.

The main pharmacokinetic parameters are summarized in Table 1. It is shown that the $AUC_{0-\tau}$ of PTX–PEG_{400}@GNP–Lips (292.71 h/mg/L) was significantly larger than those of the other two groups (66.94 h/mg/L and 137.55 h/mg/L for Taxol® and PTX–PEG_{400}@GNPs CMC-Na suspension, respectively). The MRT and $t_{1/2}$ of Taxol® (11.82 h and 6.85 h) were significantly shorter than either conjugate suspension (25.94 h and 10.16 h) or hybrid preparation (25.76 h and 14.69 h). This means that *in vivo* (1) PTX can be successfully and effectively released from hybrid liposomes and (2) the protection of liposomes could highly improve the stability of PTX and its pharmacokinetic properties, therefore enhancing the circulation longevity of the drug.

Table 1
Pharmacokinetic parameters of PTX following the *i.v.* administration of Taxol®, PTX–PEG_{400}@GNPs suspension, and PTX–PEG_{400}@GNP–Lips at the dose of 7 mg/kg in rats (mean ± SD, $n = 3$).

	Taxol®	PTX–PEG_{400}@GNPs suspension	PTX–PEG_{400}@GNP–Lips
$AUC_{0-\tau}$ (h/mg/L)[a]	66.94 ± 21.96*	137.55 ± 36.54*	292.71 ± 133.34
$t_{1/2}$ (h)[b]	6.85 ± 1.56*	10.16 ± 0.51	14.69 ± 6.86
MRT (h)[c]	11.82 ± 3.20*	25.94 ± 1.55	25.76 ± 8.12
CL (L/h/kg)[d]	0.032 ± 0.011	0.020 ± 0.0059	0.011 ± 0.0063
V_d (L/kg)[e]	0.35 ± 0.032	0.52 ± 0.17	0.24 ± 0.048

Data represent mean ± SD, n = 6.
[a] $AUC_{0-\tau}$, area under the plasma concentration–time curve from 0 to 48 h.
[b] $t_{1/2}$, plasma elimination half-life.
[c] MRT, mean residence time.
[d] CL, total body clearance.
[e] V_d, apparent volume of distribution.
* $p < 0.05$ compared with PTX–PEG_{400}@GNP–Lips.

3.5. Biodistribution

To investigate the passive targeting properties of different formulations, the biodistribution of Taxol®, PTX–PEG_{400}@GNPs CMC-Na suspension, and PTX–PEG_{400}@GNP–Lips was performed on mice and the result is shown in Fig. 6. For Taxol® and the suspension, the PTX was mainly distributed in blood, spleen and heart, while a considerable amount of PTX accumulated in the lung, liver and kidney. The apparent differences between PTX–PEG_{400}@GNP–Lips and the other two formulations is that (1) the drug elimination in blood is very slow for the hybrid liposome group and (2) the amount drug distributed into the liver increased over time. At the last test time point (12 h), the PTX concentration of PTX–PEG_{400}@GNP–Lips achieved the highest level. This value equates to an 18.2- and 5.6-fold difference compared to Taxol® and conjugate suspension, respectively.

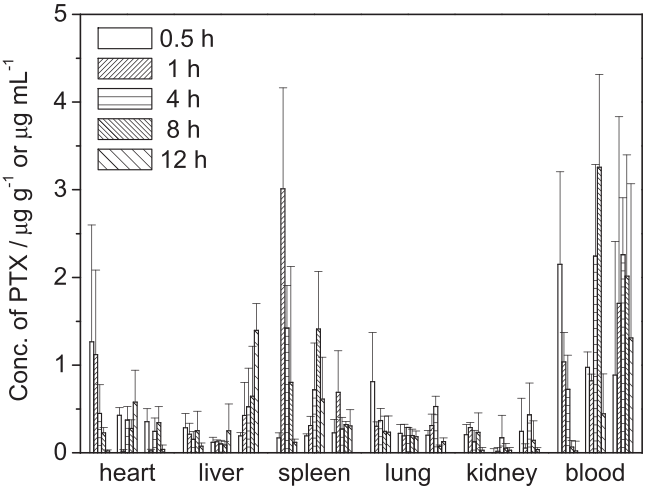

Fig. 6. The tissue distribution graphs of the three preparations (from left to right are: Taxol®, PTX–PEG_{400}@GNPs CMC-Na suspension, and PTX–PEG_{400}@GNPs–Lips, respectively) at 0.5, 1, 4, 8 and 12 h after the administration at a dose of 7 mg/kg (mean ± SD, $n = 5$).

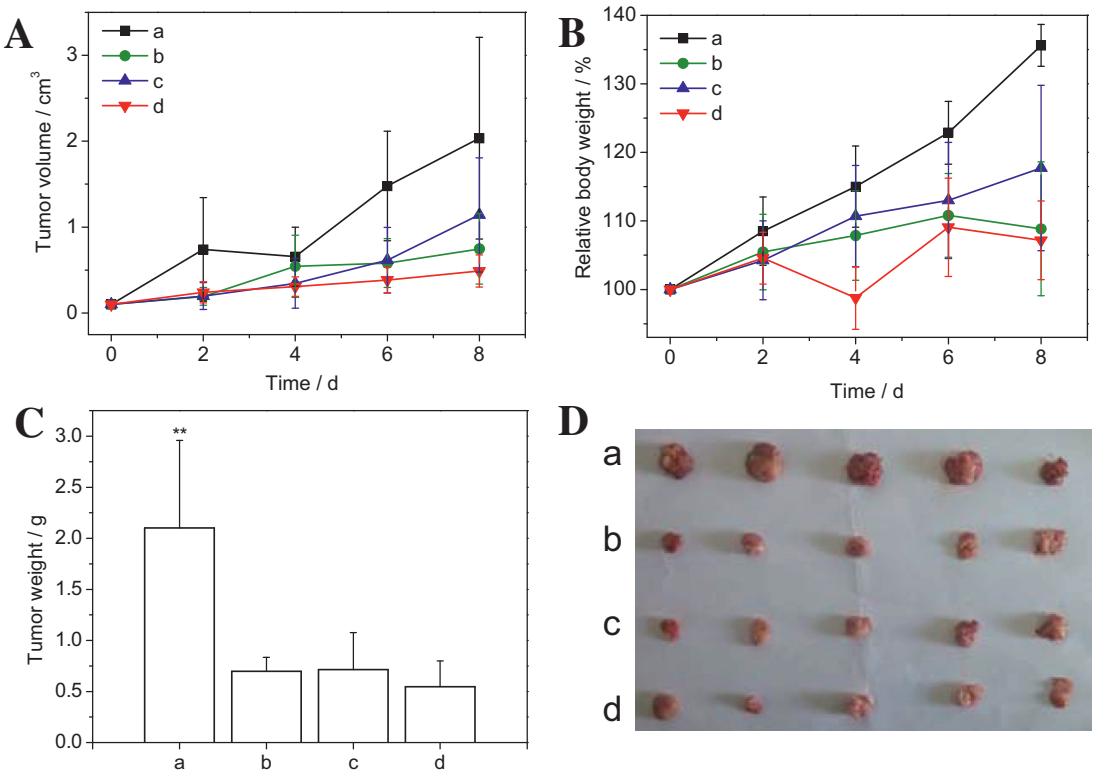

Fig. 7. (A) The relative tumor volume and (B) the relative body weight curves of each group of mice after administration, (C) the final tumor weight and (D) photograph of each group of mice after treatment for 8 days (mean ± SD, $n = 5$). The test formulations: (a) saline, (b) Taxol®, (c) PTX–PEG_{400}@GNPs CMC-Na suspension, and (d) PTX–PEG_{400}@GNP–Lips.

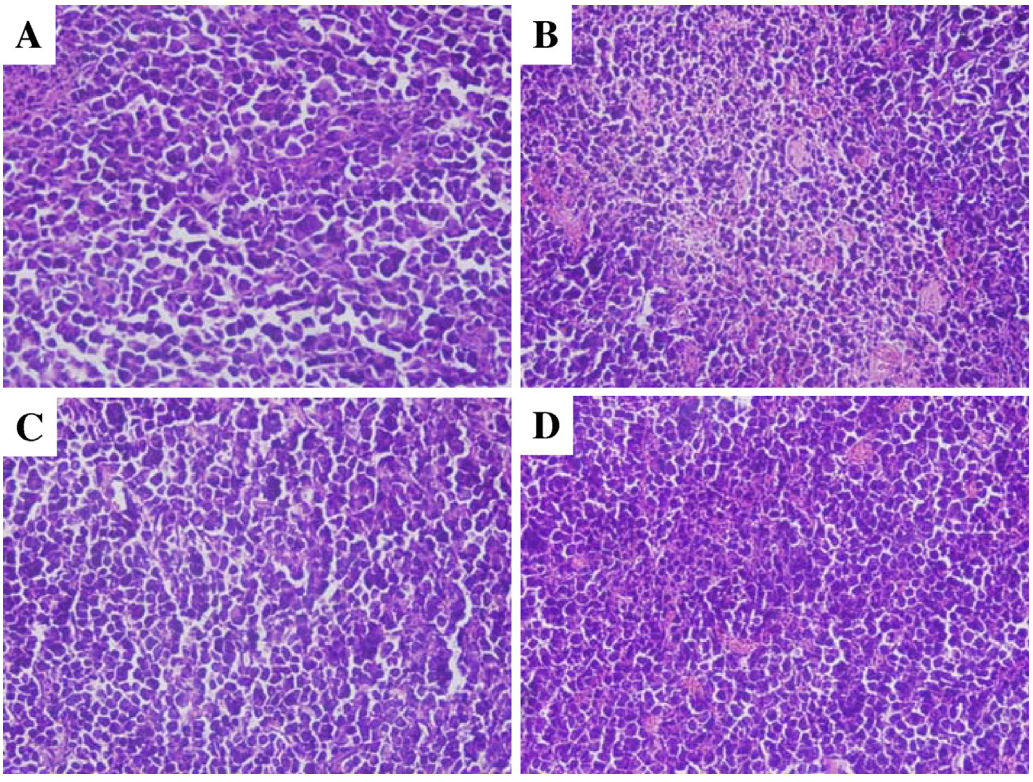

Fig. 8. The histological images of tumors sectioned and stained with H&E from different groups: (A) saline, (B) Taxol®, (C) PTX–PEG_{400}@GNPs CMC-Na suspension, and (D) PTX–PEG_{400}@GNP–Lips.

The results indicated that PTX–PEG_{400}@GNP–Lips could be beneficial to prolong the longevity of the drug in circulation and effectively target passively in the liver.

3.6. Anticancer efficacy study

To evaluate the therapeutic efficacy of hybrid liposomes on liver cancer, three formulations of PTX were administered into Heps tumor-bearing mice. Saline was used as the control and results of all samples are shown in Fig. 7. Every group had significant capability in inhibiting tumor growth when compared with the saline group, and the PTX–PEG_{400}@GNP–Lips displayed a greater decrease in body weight, tumor volume and tumor weight. This is an indication of better efficacy in liver cancer treatment, but this result shows no significance when compared with other formulations in statistics. Although hybrid liposomes showed enhanced blood PTX concentration from the very beginning as well as improved pharmacokinetic parameters, it is noticed that the drug accumulation in liver increased over time. During the test time of this work (in 12 h), the PTX concentration of PTX–PEG_{400}@GNP–Lip group in liver has not reached its maximum yet. This phenomenon indicates that the efficacy of PTX–PEG_{400}@GNP–Lips will take longer study time, which is due to their gradually passive target character and slow PTX release from this hybrid system. Therefore, this hybrid system is desirable to construct a super long-acting drug delivery system of antineoplastics.

3.7. Histological analysis

Furthermore, the tumors of each group underwent histological analysis as shown in Fig. 8. It was evident that every preparation could damage the tumor cells, while the saline group circulated without any necrosis of tumor cells. The results revealed the antitumor efficacy of the three different preparations, which was consistent with the anticancer efficacy study data mentioned and analyzed above.

4. Conclusion

Liposomes and GNPs have been employed as the model systems to construct a hybrid liposome in order to investigate the performance of chemotherapeutics transported by combinative DDSs that are composed of organic and inorganic nanomaterials. Unlike previous reports, both systems act as drug carriers at the same time. Antineoplastic PTX is covalently conjugated on the surface of GNPs, which play the role of a direct carrier. The drug-conjugated GNPs are then encapsulated in the bilayer of liposomes, which act as the second carrier to protect the conjugate system. The hybrid liposomes designed in this paper maintain the selectively intracellular and sustained drug release of gold conjugate. At the same time, the solubility, *in vivo* stability, and liver target performances of hybrid liposomes have been improved compared to the gold conjugates before the protection by liposomes. The improved circulation longevity and liver targetability not only afford the hybrid liposomes better antitumor treatment efficacy in the tumor bearing mice presented in this paper, but also provide a great possibility to develop a super long-acting drug delivery system of antineoplastics. The related research is being undertaken by our group.

Acknowledgement

This work was financially supported by the Natural Science Foundation of China (31470916), the Program for New Century Excellent Talents in University (NCET-10-0816), the Fundamental Research Funds for the Central Universities (JKQ2009026, JKP2011008), A Project Funded by the Priority Academic Program Development of Jiangsu Higher Education Institutions, and the Open Project Program of MOE Key Laboratory of Drug Quality Control and Pharmacovigilance (MKLDP2013MS04).

References

Bertrand, N., Wu, J., Xu, X., Kamaly, N., Farokhzad, O.C., 2014. Cancer nanotechnology: the impact of passive and active targeting in the era of modern cancer biology. Adv. Drug Delivery Rev. 66, 2–25.
Chakravarthy, K.V., Davidson, B.A., 2011. Doxorubicin-conjugated quantum dots to target alveolar macrophages and inflammation. Nanomed. Nanotechnol. 7, 88–96.
Daniel, M.C., Astruc, D., 2004. Gold nanoparticles: assembly, supramolecular chemistry, quantum-size-related properties, and applications toward biology catalysis and nanotechnology. Chem. Rev. 104, 293–346.
Derycke, A.S.L., Witte, P.A.M., 2004. Liposomes for photodynamic therapy. Adv. Drug Deliv. Rev. 56, 17–30.
Ding, Y., Xia, X.H., Zhai, H.S., 2007. Reversible assembly and disassembly of gold nanoparticles directed by a zwitterionic polymer. Chem. Eur. J. 13, 4197–4302.
Ding, Y., Gu, G., Xia, X.H., 2009. Cysteine-grafted chitosan-mediated gold nanoparticle assembly: from nanochains to microcubes. J. Mater. Chem. 19, 795–799.
Ding, Y., Zhou, Y.Y., Chen, H., Geng, D.D., Wu, D.Y., Hong, J., Shen, W.B., Hang, T.J., Zhang, C., 2013. The performance of thiol-terminated PEG–paclitaxel–conjugated gold nanoparticles. Biomaterials 34, 10217–10227.
Ding, Y., Jiang, Z., Saha, K., Kim, C.S., Kim, S.T., Landis, R.F., Rotello, V.M., 2014a. Gold nanoparticles for nucleic acid delivery. Mol. Ther. 22, 1075–1083.
Ding, Y., Liang, J.J., Liu, Z.Y., Wu, D., Dong, L., Xia, X.H., Shen, W.B., Zhang, C., 2014b. Development of a liver-targeting gold-PEG-galactose nanoparticle platform and the structure-function study. Part. Part. Syst. Charact. 31, 347–356.
Farokhzad, O.C., Langer, R., 2009. Impact of nanotechnology on drug delivery. ACS Nano 3, 16–20.
Gui, R., Wan, A., Liu, X., Jin, H., 2014. Intracellular fluorescent thermometry and photothermal-triggered drug release developed from gold nanoclusters and doxorubicin dual-loaded liposomes. Chem. Commun. 50, 1546–1548.
Jang, H.R., Oh, H.J., Kim, J.H., Jung, K.Y., 2013. Synthesis of mesoporous spherical silica via spray pyrolysis: Pore size control and evaluation of performance in paclitaxel pre-purification. Microporous Mesoporous Mater. 165, 219–227.
Kataoka, K., Harada, A., Nagasaki, Y., 2001. Block copolymer micelles for drug delivery: design, characterization and biological significance. Adv. Drug Deliv. Rev. 47, 113–131.
Lasic, D.D., Templeton, N.S., 1996. Liposomes in gene therapy. Adv. Drug Deliv. Rev. 20, 221–266.
Liang, J.J., Zhou, Y.Y., Wu, J., Ding, Y., 2014. Gold nanoparticle-based drug delivery platform for antineoplastic chemotherapy. Curr. Drug Met doi:http://dx.doi.org/10.2174/1389200215666140605131427.
Liao, C., Sun, Q., Liang, B., Shen, J., Shuai, X., 2011. Targeting EGFR-overexpressing tumor cells using cetuximab-immunomicelles loaded with doxorubicin and superparamagnetic iron oxide. Eur. J. Radiol. 80, 699–705.
Liu, Z., Chen, K., Davis, C., 2008. Drug delivery with carbon nanotubes for in vivo cancer treatment. Cancer Res. 68, 6652–6660.
Liu, D.H., Liu, F.X., Liu, Z.H., Wang, L.L., Zhang, N., 2011. Tumor specific delivery and therapy by double-targeted nanostructured lipid carriers with anti-VEGFR-2 antibody. Mol. Pharm. 8, 2291–2301.
Oh, J., Yoon, H.J., Park, J.H., 2014. Plasmonic liposomes for synergistic photodynamic and photothermal therapy. J. Mater. Chem. B 2, 2592–2597.
Rengan, A.K., Jagtap, M., De, A., Banerjee, R., Srivastava, R., 2014. Multifunctional gold coated thermo-sensitive liposomes for multimodal imaging and photothermal therapy of breast cancer cells. Nanoscale 6, 916–923.
Samad, A., Sultana, Y., Aqil, M., 2007. Liposomal drug delivery systems: an update review. Curr. Drug Deliv. 4, 297–305.
Sinha, R., Kim, G.J., Nie, S., Shin, D.M., 2006. Nanotechnology in cancer therapeutics: bioconjugated nanoparticles for drug trun 0delivery. Mol. Cancer Ther. 5, 1909–1917.
Torchilin, V.P., 2005. Recent advances with liposomes as pharmaceutical carriers. Nat. Rev. Drug Discov. 4, 145–160.
Wu, J., Kamly, N., Shi, J., Zhao, L., Xiao, Z., Hollett, G., John, R., Ray, S., Xu, X., Zhang, X., Kantoff, P.W., Farokhzad, O.C., 2014. Development of multinuclear polymeric nanoparticles as robust protein nanocarriers. Angew. Chem. Int. Ed. 53, 8975–8979.